

**Title:**

Universal scaling of the critical temperature for thin films near the superconducting-to-insulating transition

**Authors:**

Yachin Ivry,<sup>1\*</sup> Chung-Soo Kim,<sup>1</sup> Andrew E. Dane,<sup>1</sup> Domenico De Fazio,<sup>1,2</sup> Adam McCaughan,<sup>1</sup> Kristen A. Sunter,<sup>1</sup> Qingyuan Zhao<sup>1</sup> and Karl K. Berggren.<sup>1\*</sup>

**Affiliations:**

<sup>1</sup> Research Laboratory of Electronics, Massachusetts Institute of Technology, 77 Massachusetts Avenue, Cambridge, Massachusetts 02139, USA.

<sup>2</sup> Department of Electronics and Telecommunications (DET), Polytechnic University of Turin, Corso Duca degli Abruzzi 24, 10129 Torino, Italy.

\* Correspondence to: berggren@mit.edu, ivry@mit.edu.

Abstract:

**Thin superconducting films form a unique platform for geometrically-confined, strongly-interacting electrons. They allow an inherent competition between disorder and superconductivity, which in turn enables the intriguing superconducting-to-insulator transition and believed to facilitate the comprehension of high- $T_c$  superconductivity. Furthermore, understanding thin film superconductivity is technologically essential *e.g.* for photo-detectors, and quantum-computers. Consequently, the absence of an established universal relationships between critical temperature ( $T_c$ ), film thickness ( $d$ ) and sheet resistance ( $R_s$ ) hinders both our understanding of the onset of the superconductivity and the development of miniaturised superconducting devices. We report that in thin films, superconductivity scales as  $dT_c(R_s)$ . We demonstrated this scaling by analysing the data published over the past 46 years for different materials (and facilitated this database for further analysis). Moreover, we experimentally confirmed the discovered scaling for NbN films, quantified it with a power law, explored its possible origin and demonstrated its usefulness for superconducting film-based devices.**

Relationships between low-temperature and normal-state properties are crucial for understanding superconductivity. For instance, the Bardeen-Cooper-Schrieffer theory (BCS) successfully associates the normal-to-superconducting transition temperature,  $T_c$ , with material parameters, such as the Debye temperature ( $\Theta_D$ ) and the density of states at the Fermi level ( $N(0)$ ). Hence, the BCS model allows us to infer superconducting characteristics (*i.e.*  $T_c$ ) from properties measured at higher temperatures [1]. In the BCS framework, superconductivity occurs when attractive phonon-mediated electron-electron interactions overcome the Coulomb repulsion, giving rise to paired electrons (Cooper pairs) with a binding energy gap:  $\Delta$ . Moreover, within a superconductor,

all Cooper pairs are coupled, giving rise to a collective electron interaction. Such a collective state is described by a complex global order parameter with real amplitude ( $\Delta$ ) and phase ( $\phi$ ):  $\Psi = \Delta e^{i\phi}$ .

Since superconductivity relies on a collective electron behaviour, the onset of superconductivity occurs when the number of participating electrons is just enough to be considered collective, *i.e.* at the nanoscale [2–5]. Thus, it is known that the superconductivity-disorder interplay varies in thin films and is effectively tuned with the film thickness ( $d$ ) or with the disorder in the system, which is represented by sheet resistance of the film at the normal state ( $R_s$ ) [6–10]. The mechanism of superconductivity in thin films has been investigated since the 1930s [11]. The development of thin film growth methods in the late 1960s allowed Cohen and Abeles to demonstrate an increase in  $T_c$  with decreasing thickness in aluminium films in a study that pioneered the currently ongoing research of thin superconducting films [12]. This enhancement of  $T_c$ , which is still not completely understood, was later confirmed by Strongin *et al.* [13], who reported also the more common behaviour of  $T_c$ —its suppression with reduced film thickness. Strongin *et al.* empirically examined different scaling options for the observed suppression of  $T_c$  in lead and suggested that  $T_c$  scales with  $R_s$  better than it does with the other parameters, such as the film thickness. This suggestion, is still influential on the data analysis done in the field today and it encouraged the derivation of theoretical models to explain a dependence of  $T_c$  on  $R_s$ . Indeed, Beasley *et al.* (followed by Halperin and Nelson) derived that  $T_c$  depends only on  $R_s$  for a Berezinsky-Kosterlitz-Thouless (BKT) transition, in which vortex-antivortex pairs, and not Cooper pairs, dominate the transition, which in turn is universal in nature [8,14]. In addition, the mathematical derivation of the interacting-boson treatment within the BKT framework was also used in a reminiscent framework that associates interacting paddles of Cooper pairs with a multiple-Josephson Junction array [15]. Likewise, Finkel'stein used renormalisation group tools to derive exactly a different expression

for the dependence of  $T_c$  on  $R_s$  (with no direct dependence on the thickness). This derivation was based on a modified BCS equation, in which mean field theory was integrated with homogeneous disorder *i.e.* impurity scattering due to Coulomb and spin density interactions [9]. As opposed to these three models that claim that  $T_c$  depends merely on  $R_s$ , competing models, such as the proximity effect [7] and the quantum size effect [10] theories suggest that  $T_c$  depends on  $d$  only, with no direct dependence on  $R_s$ . Nevertheless, none of these models is sufficient to explain the entirety of the accumulated experimental data [12,13,16–29] despite the long-standing attempt to do so either through a direct mathematical derivation as in the above model, or with the aid of empirical universal laws [30].

Relationships between  $d$ ,  $R_s$  and  $T_c$  are significant even to a broader scope than thin superconducting films. That is, the dependencies  $T_c(d)$  and  $T_c(R_s)$  are important for superconducting films. However, the dependence of resistivity ( $\rho \equiv dR_s$ ) on film thickness in thin metallic films has also occupied both scientists and technologists for many decades. Since above  $T_c$  the superconducting films behave like normal metals, the relationship  $R_s(d)$  is similar to that of normal metals. That is, presumably, the resistivity is expected to remain constant or to demonstrate a smooth minor monotonic increase with reduced film thickness. Therefore, it is not important if  $T_c$  is expressed as a function of  $d$  or of  $R_s$ , as presumably, one parameter can be replaced by the other straightforwardly. Theoretically, the relationship  $\rho(d)$  is usually discussed in terms of derivatives of the Fuchs's theory [31], sometimes combined with Matthiessen's rule [32]. However, surprisingly, to-date, the existing theories encounter difficulties in fitting the experimental data which are often scattered when plotted on a  $\rho(d)$  graph [33]. In addition to challenging our understanding of metallic thin films, such scatter prevents a smooth quantitatively valuable transition between descriptions of  $T_c(R_s)$  and  $T_c(d)$  in the case of superconductors.

A seminal experimental work by Goldman and co-authors [21] suggested that beyond certain film thickness or sheet resistance values  $T_c$  is suppressed so much that practically, the material will never become superconducting. That is, the cooling curves of such thin films indicate that  $R_s$  increases with decreasing temperature—a behaviour that is typical in insulators and not in metals. This observation began the race to understanding the superconducting-to-insulator phase transition, which is believed by many researchers to be of a quantum nature [5]. To date, although much data for thin film superconductivity have been accumulated [12,13,16–29] and the local disorder has already been observed directly [34], the mechanisms governing the collective behaviour close to the superconducting-to-insulating transition, or near the onset of superconductivity have remained elusive. That is, a model equivalent to the BCS but that is valid for thin films, is still missing. Specifically, the theories that suggest that  $T_c$  varies with either  $R_s$  or  $d$  are material dependent, while for some materials, none of the existing theories agrees with the observations. The absence of a unified description of superconductivity in thin films is even more pronounced when bearing in mind that the onset of superconductivity in such geometries is believed to occur through a quantum phase transition, which is in principle universal. Moreover, understanding superconductivity in thin films is expected to clarify the behaviour of resistance in thin metallic films in general. Likewise, it has even been suggested that the superconductivity-disorder interplay in thin films is the key for understanding high- $T_c$  superconductivity [4]. Therefore, it is the goal of this paper to demonstrate a universal behaviour for  $T_c$  in thin films as a function of both  $d$  and  $R_s$ .

In addition to the scientific impact associated with understanding superconductivity in thin films, thin superconducting films are of a great technological significance as they are the basis for most miniaturised superconducting devices [35,36]. In particular, quantum-based technologies, such as

computation, encryption and communication rely on such films. Similarly, the leading technology for sensing single photons fast [37] and at a broad spectral range [38]--superconducting nanowire single photon detectors (SNSPDs)--is also based on thin superconducting films [39]. Nevertheless, the lack of understanding of the underlying mechanism of superconductivity in thin films and the large scatter of the experimental data for the relationships between  $T_c$ ,  $R_s$  and  $d$  typically lead to low confidence in the film growth process, encumbering the relevant technological developments. Specifically, the limited reproducibility and control of the film parameters impair both the yield and the size of devices made out of such films. For instance, the yield of SNSPDs made out of thin niobium nitride (NbN) films is low, while their active area is usually restricted, hindering the technological advances in the field. Hence, a universal scaling of the properties of thin superconducting films is expected to improve the control and reproducibility of the film properties, and therefore, to allow at last realisation of the potential of miniaturised superconducting devices.

We show that for a given material, the relationship between film thickness, sheet resistance and critical temperature scales as  $dT_c(R_s)$ . Moreover, this scaling typically follows a power law. We demonstrated the scaling on data gathered from some thirty different sets of materials published since 1968, which cover most of the literature. The materials studied included clean, dirty, granular, and amorphous superconductors. Some of these materials are type I in their bulk state, and some are type II. Most of these materials exhibited suppression of  $T_c$  at reduced thicknesses, but some exhibited enhancement. The data in its entirety could not fit previous theories [7–10], but did fit the new power-law relationship across broad range of  $T_c$ ,  $d$  and  $R_s$ . We extracted the coefficient and exponent of the power law for each material, and demonstrated that the coefficient and the exponent are correlated. The power law fits the data from materials that fit also one of the previous models  $T_c(d)$  or  $T_c(R_s)$ , as well as for materials that presumably are not BCS. We also

examined our own new experimental data on NbN thin films. In these data, relating  $dT_c$  to  $R_s$  provided fits with reduced scatter relative to fits suggested by previous models [7–10,31–33]. Finally, we supply two possible explanations of the observed universal behaviour. We should note that the data gathered from the literature is available for further review in the Supplemental Material [40].

To illustrate the new scaling, we will start by examining our data on NbN films. We chose sputtered NbN as the material for this study for four main reasons: (a) it is widely researched, and experimental data collected for different growth methods and conditions are available; (b) there are contradicting reports about which of the existing models describes the  $T_c$  suppression in NbN films. For instance, Kang *et al.* claimed that  $T_c$  is suppressed due the quantum size effect [19], Wang and co-authors suggested that the suppression follows Finkel'stein's model [18], Semenov *et al.* determined that the suppression is governed by the proximity effect [20] and Koushik *et al.* argued that the transition is of a BKT type [41]; (c) the relatively high  $T_c$  of NbN (16 K for a bulk NbN [42]) assists the experimental investigation; and (d) its properties make it useful for photodetectors [35,37,43,44].

Figures 1a and 1b show the dependence of  $T_c$  on thickness and on sheet resistance for our NbN films, allowing a comparison of the data with the existing models [7–10,31–33]. Although a general trend can be seen in both  $T_c(d)$  and  $T_c(R_s)$ , the scatter in these graphs is too large to allow confident fitting to any model of the form  $T_c(d)$  or  $T_c(R_s)$ . Bearing in mind the metallic characteristic of the films, the resistivity of the grown films corresponds to their inverse mean free path and hence should increase monotonically with decreasing thickness [31]. However, Fig. 1c shows the dependence of resistivity on thickness in our films, revealing again, large scatter of the data points with only vaguely the expected trend (as a side remark we should note that the regime

in which the scatter is the largest is when the thickness is around 6 nm, which is the nominal coherence length of NbN films [20]).

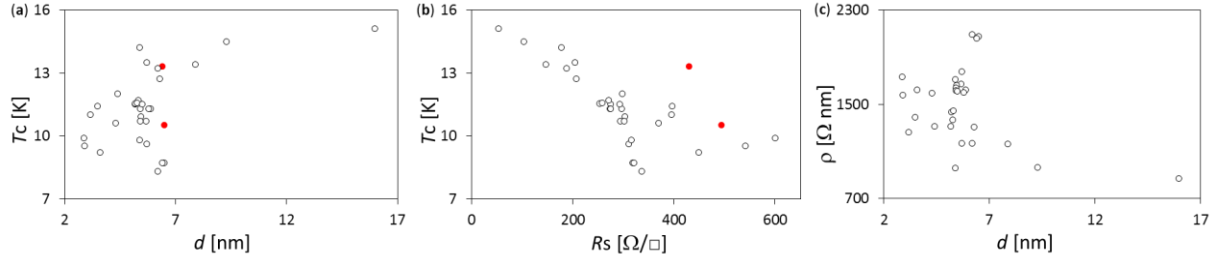


**Figure 1| Metallic and superconducting behaviour of thin NbN films.** (a) Critical temperature of NbN films as a function of the film thickness ( $d$ ) and (b) sheet resistance ( $R_s$ ) indicates no clear correlation with general functions of the form  $T_c(R_s)$  or  $T_c(d)$ . (c) Resistivity ( $\rho \equiv R_s \cdot d$ ) of the NbN films vs. thickness reveals a scattered data set. Chemical treatment of the substrate prior to deposition is suspected of influencing the properties of the red solid points here and in Fig. 3, while their high resistivity is outside the range presented in Fig. 1c but is discussed in the Supplemental Material [40].

One potential possible origin for the large scatter and for the deviation from a clear trend of the curves  $T_c(d)$  or  $T_c(R_s)$  in our NbN films is low material quality that might stem *e.g.* from extensive granularity, poor crystallinity, large strain etc. To avoid such effects and to obtain high material quality, we grew the NbN films on MgO substrates, with which the lattice mismatch is small (< 3.5%). Moreover, during the deposition, we heated the substrate to a nominal temperature of 800° C to further improve the crystallographic growth by relaxing the deposited film. We also used a system with a low base pressure ( $4.5\text{-}9 \cdot 10^{-9}$  Torr), minimising the magnetic and other impurities in the films. To determine the quality of our NbN films, we demonstrated (Fig. 2a) with transition electron microscopy (TEM) that our NbN films are grown epitaxially on the MgO substrate,

forming highly-orientated crystallinity, *i.e.* clear long range cubic structure with low level of granularity, if exists at all (we examined with TEM representative films, see Methods for details). In addition to the atomic resolution TEM imaging, the highly-orientated crystallinity of the NbN films and the good lattice matching between the NbN and the MgO substrate were observed also in the selective area electron diffraction (Fig. 2b). Furthermore, the measured lattice constant of the cubic NbN films is very close to the literature value, suggesting the films are relaxed.

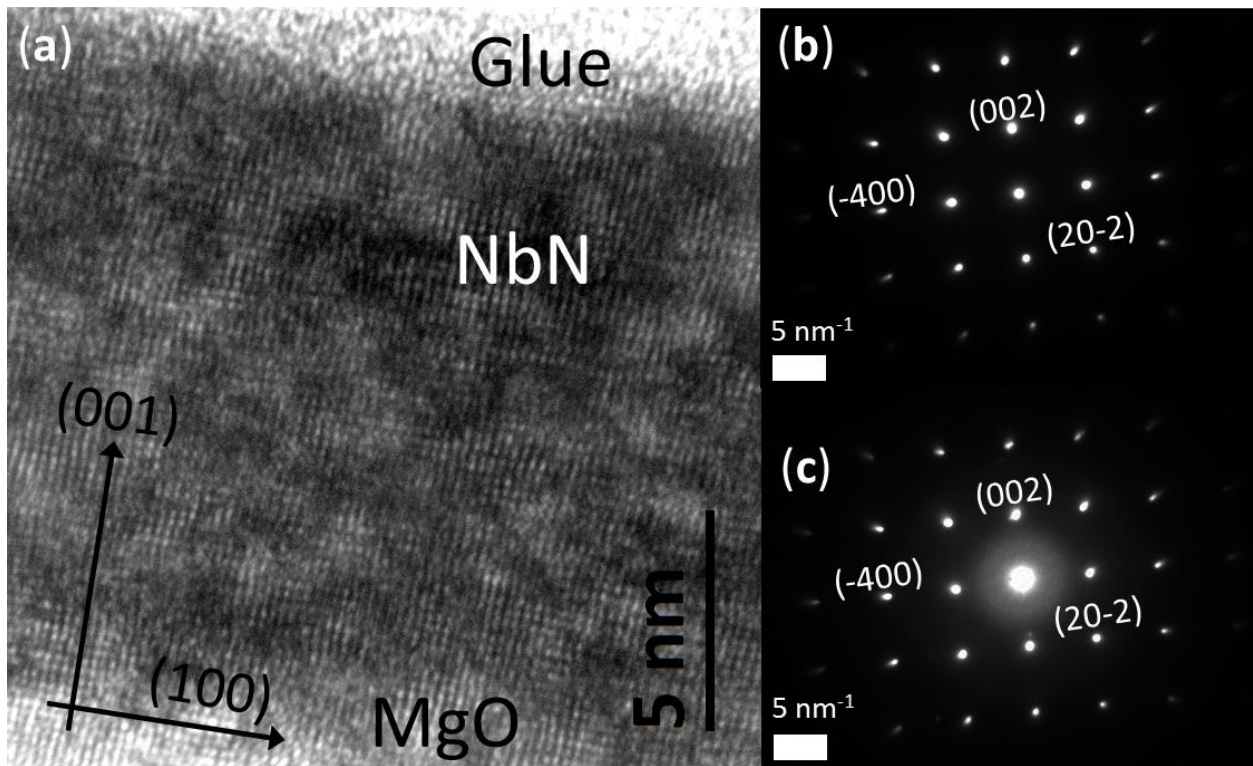


**Figure 2| TEM micrographs of epitaxial NbN film on an MgO substrate.** (a) Atomic structure of an NbN film on an MgO substrate, demonstrating epitaxial growth of long-range cubic structure and good lattice matching with the substrate. The lattice constants of both MgO and NbN are  $4.35 \pm 0.1 \text{ \AA}$ . (b) Selective area electron diffraction from an area within the MgO substrate only and (c) from an area that spans the MgO substrate, NbN film and the glue layer (that is used to protect the film from the top) demonstrates high crystallinity of both the MgO and NbN and a good lattice

matching between these substances. The bright spot in the centre of (c) is due to the amorphous glue.

Given that the epitaxial films were of high quality and that they were grown under similar conditions, the fact that Fig. 1 failed to show any clear correlations between the parameters  $d$ ,  $R_s$  and  $T_c$  suggests that a different scaling method is required. Since  $T_c$  is usually suppressed with reduced thickness and with the increase in disorder (*i.e.* with increasing  $R_s$ ), we examined the relationship  $dT_c$  as a function of  $R_s$ . Indeed, Fig. 3 shows that plotting  $dT_c$  vs.  $R_s$  reveals a clear trend, while the scatter was reduced significantly with respect to the traditional scaling curves that were presented in Fig. 1. This decrease in scatter is even more remarkable when taking into account that when multiplying two parameters that were measured independently (*i.e.* thickness and  $T_c$ ) the statistical noise should increase, and not decrease.

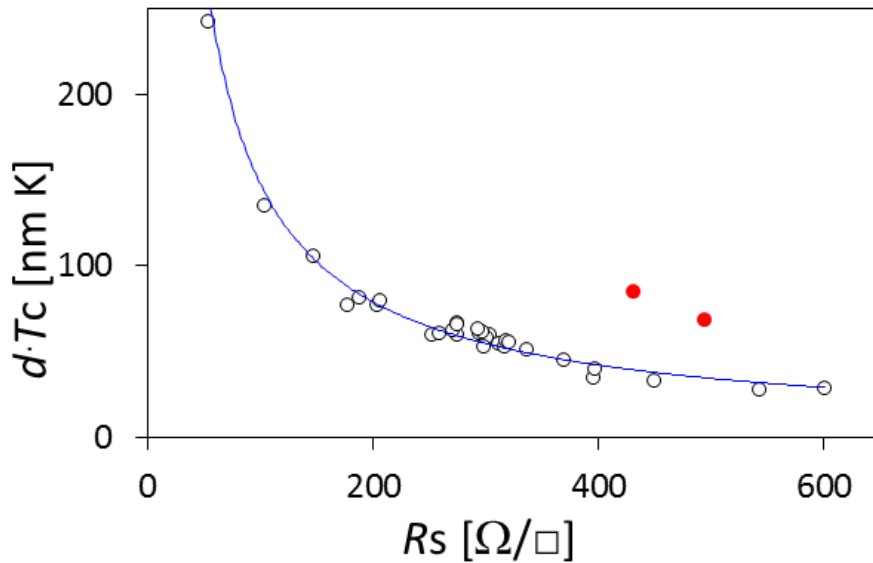


**Figure 3| Fitting our NbN on MgO data to the power law  $dT_c(R_s)$ .** (a) Plotting  $dT_c$  vs.  $R_s$  for the NbN films reduces the scattering significantly with respect to the curves in Fig. 1. The blue

line is the best fit to Eq. 1 ( $A = 9448.1$  and  $B = 0.903$ ). Red solid points are discussed in the Supplementary Material [40].

The blue solid line in Fig. 3 was added not only to guide the eye for the clear trend and reduced scatter with respect to Fig. 1, but this line is also the best fit of the data to the power law:

$$dT_c = A \cdot R_s^{-B} \quad (\text{Eq. 1})$$

where  $A$  and  $B$  are fitting parameters and hereafter  $d$ ,  $T_c$  and  $R_s$  are unitless when the appropriate values are given in nm, K and  $\Omega/\square$ . The exponent  $B$  in Fig. 3 is close to unity ( $B \approx 0.9$ ) so technically, one can approximate Eq. 1 to a reduced form:  $\rho \cdot T_c \sim \text{constant}$ . Yet, when using Eq. 1 to predict the  $T_c$  of a film [40], the exponent  $B$  is needed.

We can suggest two approaches to explain the origin of Eq. 1. The first approach is based on the BCS-related models. Specifically, one can rewrite Eq. 1 as:

$$T_c = (A/d) \cdot e^{-B \ln(R_s)} \quad (\text{Eq. 2a})$$

Bearing in mind the BCS-based frameworks, Eq. 2a is written in a similar form to these equations *i.e.*  $T_c$  equals to an amplitude ( $A/d$ ) times an exponent that expresses the electron interactions ( $B \cdot \ln(R_s)$ ). For instance, in the framework of the BCS-based McMillan equation [45,46] ( $T_c = \frac{\theta_D}{1.45} e^{-\frac{1.04(1+\lambda)}{\lambda-\mu^*(1+0.62\lambda)}}$ ), Eq. 2a implies that changes in  $N(0)$  or in the interaction ( $\lambda$  or  $\mu$ ) may scale as  $B \cdot \ln(R_s)$  (where  $\lambda$  and  $\mu$  are the electron-phonon coupling constant and the Coulomb repulsive interactions). This outcome is reminiscent also of Finkel'stein's derivation of  $T_c(R_s)$  for homogenous superconductors where the interaction term was also rephrased in terms of the sheet resistance (while we recall that a logarithmic accuracy was claimed in that framework), but with the main difference that here  $d$  appears explicitly [9].

The second approach to explain Eq. 1 relies on the fact that above  $T_c$ , conventional superconductors are normal metals. Thus, the relationship between  $d$  and  $R_s$  for the examined thin superconducting films is the same as that for metals in general. Hence, here, Eq. 1 implies a somewhat broader generalisation of the thickness dependence of resistance in thin metallic films. That is, one can isolate  $R_s$  as a function of  $d$  and  $T_c$ :

$$R_s = (A/dT_c)^{1/B} \quad \text{(Eq. 2b)}$$

This manipulation is justified *e.g.* if  $A$ ,  $B$  and  $T_c$  are representatives of simple material properties such as  $\Theta_D$ , mechanical strain, granularity,  $N(0)$  etc. In this case, a power-law-form thickness dependence of these properties can also explain Eq. 1. We should emphasise here that although for thick materials,  $R_s \sim 1/d$ , this is usually not true for thin films (*i.e.* when  $T_c$  deviates significantly from its bulk value), as can be seen for instance in Fig. 1c. Therefore, the fit of our data to Eq. 1 (Fig. 3) cannot be due to such simple relationships.

It is worth mentioning that Eq. 1, and more so its reduced form, resembles Homes's Law, which empirically relates  $T_c$  through the superfluid density to the normal state conductivity in the case of high- $T_c$  superconductors [3]. However, thus far, we were not able to derive a direct relationship between the two laws.

To demonstrate the full range of applicability of Eq. 1, we showed that this equation fits data gathered from the literature for  $\sim 30$  other superconductors studied over the past 46 years that summarise all of the reports from which we could extract  $d$ ,  $R_s$  and  $T_c$  [12,13,16–29]. In some cases, we merged data reported in different publications by the same authors. We should note that, although  $R_s$  can usually be measured rather accurately, the thickness, which is measured indirectly, is typically reported with a lower level of confidence [40]. Moreover, although there is an ongoing

dispute of how to determine  $T_c$  in thin films, usually the values for  $T_c$  are measured in a consistent manner within a data set of a given material, allowing an examination of each data set at least with itself [47]. These data include NbN sets of films that were reported previously by other groups, each of which were reported to be in agreement with one of the models of the form  $T_c(R_s)$  [18] or  $T_c(d)$  [19,20]. Moreover, it includes some ‘classical’ examples such as the seminal Bi films by Goldman and co-workers [21] and the homogeneous  $\alpha$ MoGe films of Graybeal *et al.* who were used for demonstrating Finkelstein’s model [9,48]. The data and analysis of each of these materials is discussed in detail on a linear scale in the Supplemental Material [40] (*e.g.* a detailed analysis of  $\alpha$ MoGe films is brought in Section S7 in the Supplemental Material [40]). We should note that in addition to the contribution of the Supplemental Material [40] to the current work, this inclusive database is available also for readers who seek further investigation of superconducting and metallic behaviour in thin films.

Although detailed analysis of the individual materials is brought in the Supplemental Material [40], the most common method to present data points that follow Eq. 1 is by linearity on a log-log scale of  $dT_c$  vs.  $R_s$ . Indeed, the linearity of the data in Fig. 4a-b clearly validates Eq. 1 for a broad range of  $T_c$ ,  $d$  and  $R_s$  (we divided the data between Fig. 4a and 4b arbitrarily to spread data that otherwise would have been too crowded to distinguish). To eliminate the possibility that the scaling of Eq. 1 is due to *e.g.* an inverse proportionality between  $R_s$  and  $d$  which by chance fits with a power law relation for  $T_c(R_s)$  or for  $T_c(d)$ , in Fig. 4c we presented the resistivity as a function of thickness for these materials. Likewise, in Fig. 4d and 4e we showed the dependence of  $T_c$  on thickness and on sheet resistance. The non-linearity and non-uniformity of the data in Fig. 5c-e emphasise the universality presented in Fig. 5a-b (we should note that the set of  $\alpha$ Nb<sub>3</sub>Ge films reported by Kes and Tsuei [24] and the thicker films of Wang and co-authors [16–18] are brought

as examples for thick films, in which both the resistivity and  $T_c$  are rather constants over the entire range of thickness reported for these films. However, it is clear from Fig. 4 that this is not the case for all the other data sets). In addition, the complete presentation of the individual sets of data on a linear scale in the Supplementary Material [40], demonstrates that Eq. 1 quantitatively fits well the data from each material. This exhaustive list that surveys thin-film superconductors and presents their properties also includes some superconductors that require more gentle treatment, for instance, superconductors that only qualitatively agree with the scaling  $dT_c$  vs.  $R_s$  (e.g.  $MgB_2$  [49]) as well as the few material sets that do not exhibit convincing agreement with this scaling (Ga [50], Sn [13],  $Nb_3Sn$  and  $V_3Si$  [51]).

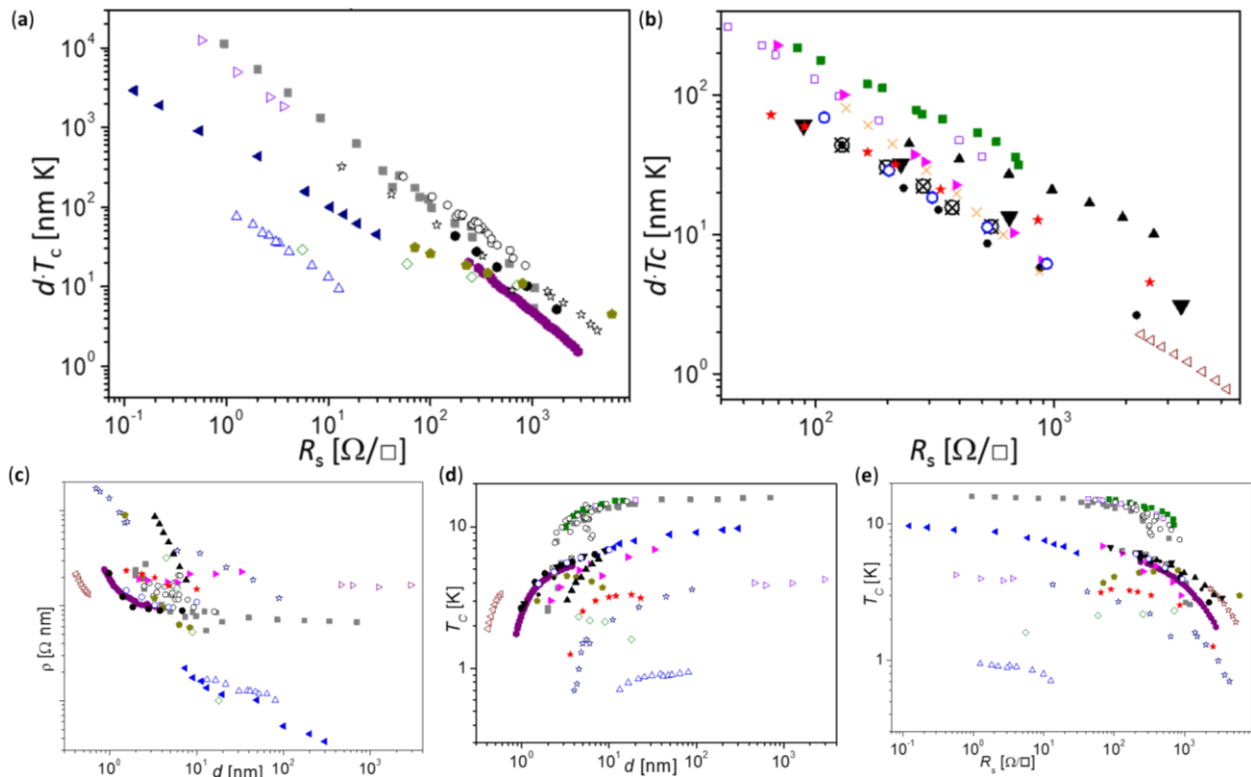


**Figure 4| Scaling of superconducting and metallic properties in thin films.** (a) and (b) show the dependence of  $dT_c$  on  $R_s$  for various superconductors (data sets are arbitrarily split to two panels to prevent indistinguishability). The linearity of the data on a log-log scale is in good

agreement with Eq. 1. (c) Resistivity dependence on thickness for representative materials (log-log scale). (d)  $T_c$  as a function of thickness and (e) of sheet resistance of these materials on log-log scales. The following symbols were used in (a-f): ■-NbN from Wang and co-authors [16–18]; ■-NbN by Semenov *et al.* [20]; □-NbN by Kang *et al.* [19]; ○-our NbN films (from Fig. 1); △-Mo [52]; ●-Bi and ◁-Pb by Haviland, Liu and Goldman [21]; ◇-Al from Cohen and Abeles [12]; ◀-Nb [53]; ☆-disordered TiN by Klapwijk and co-authors [22,23]; ★- disordered TiN by Baturina and co-authors [54]; ▷- $\alpha$ Nb<sub>3</sub>Ge [24]; ✕- $\alpha$ MoGe from Graybeale and Beasley [55]; ►- $\alpha$ MoGe from Graybeal and co-authors [25–27]; ◆- $\alpha$ MoGe by Yazdani and Kapitulnik [28]; ✱- $\alpha$ ReW by Raffy *et al.* [29]; while ◆ is Al, and ▼, ▲, ⊕, ●, • and ○ are Pb films, corresponding to the same symbols used in Strongin *et al.* [13]. A complete list of the data is given in the Supplemental Material [40].

To allow further examination of the universality presented in Fig. 4a-b, we plotted in Fig. 5a the intercepts of the different curves as a function of their slopes ( $A$  vs.  $B$  in Eq. 1). In this way, each material is represented by a single data point, allowing a comparison between the different superconductors. Figure 5a shows that the data points follow a general trend, so that  $A$  and  $B$  are correlated. It is interesting to note that the materials at the two extreme points of this curve are aluminium (in which  $T_c$  is enhanced in thin films) and  $\alpha$ MoGe, implying that  $A$  and  $B$  may be determined by the granularity of the superconductor. In fact, since the interaction in Eq. 2a is reminiscent of Finkelstein’s model, which is turn had no implicit dependence on thickness and is valid for homogeneous (amorphous) superconductors, Fig. 5a suggests that the thickness-dependent coefficient is more significant to granular films, while for amorphous films, the  $R_s$ -based interaction is dominating. Further discussion about the potential relationship between  $A$  and  $B$  can be found in the Supplemental Material (mainly in Sections S7.1 and in S17) [40].

Independently, the data aggregation around  $B = 1$  indicates that  $\rho T_c \sim \text{constant}$  is a reasonable approximation in several cases. More specifically, the histogram in Fig. 5b suggests that  $B \approx 0.9$  to 1.1 is a universal exponent that represents the scaling of Eq. 1. In fact, a correlation between the coefficient and the exponent such as the one observed in Fig. 5a indicates that a logarithmic correction to the power law may support universality of the exponent  $B \approx 0.95$ . We should note that a universal value of  $B$  (e.g.  $B = 0.95$ ) means that this may help describing superconductivity in thin films in general, but it does not mean that such a value is a good approximation for any of the specific materials.

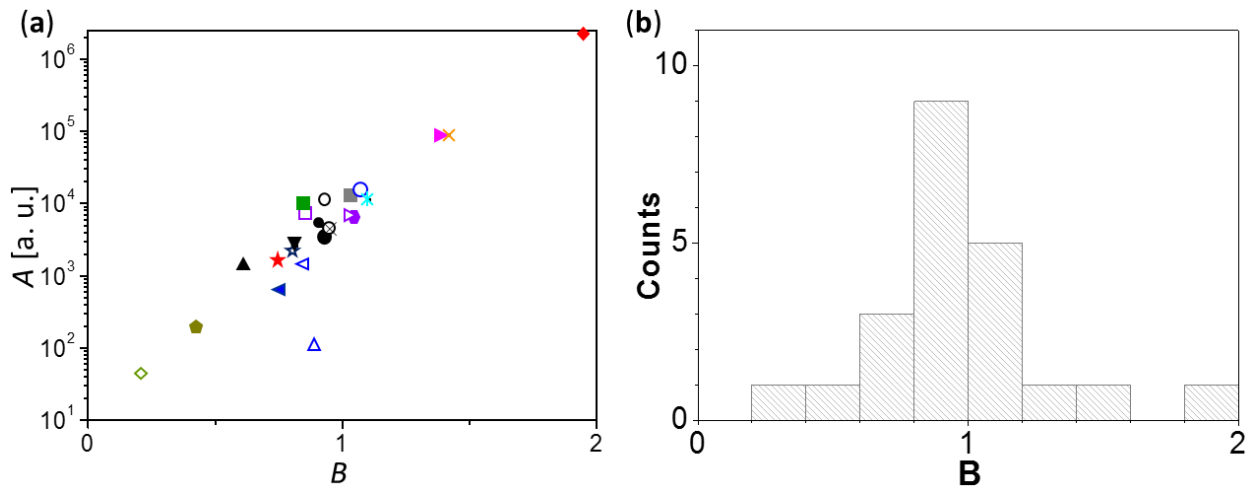


**Figure 5| Universality of the scaling  $d \cdot T_c(R_s)$ .** (a) Intercept versus slope ( $A$  vs.  $B$  with respect to Eq. 1) of the best linear fits for the graphs in Fig. 4a-b suggests that the parameters  $A$  and  $B$  are correlated (for details, see S7 and S17 in [40]). Legend corresponds to Fig. 4, while the only material outside the trend ( $\triangle$ ) is molybdenum. (b) histogram of the exponents  $B$  with a mean value at  $B \approx 0.95$ .

It often occurs that one or more films in a data set are different than the others *e.g.* due to faults in the growth process. In many cases, it is difficult to identify such a film in a  $T_c(R_s)$  or in a  $T_c(d)$  curve. Therefore, the confidence in determining whether the growing system is stable or not is

low. This lack of confidence obstructs the relevant scientific studies. Furthermore, it affects very badly the ability to reliably fabricate miniaturised superconducting devices. The solid red points in our own data in Figures 1 and 3 and two films from Semenov *et al.* [20] are examples, and are discussed in detail in the Supplementary Material [40] (Sections S11.5 and S11.2). Since such films stand out on a  $dT_c(R_s)$  curve, we propose to use this scaling as a practical method to assess the quality of superconducting films. Moreover, once the parameters  $A$  and  $B$  in Eq. 1 are determined for a specific set of films,  $T_c$  can be derived from measurements that are done in the normal state (*e.g.* at room temperature). Indeed, using the scaling law of Eq. 1 we were able to better control and evaluate our growth system. This control helped us in increasing the yield of SNSPDs made in our group. Moreover, the improvement of control of the film properties allowed us to make larger area, and hence more advanced nano-superconducting devices [56,57]. In addition, the analysis done with Eq. 1 also proved useful to predict the behaviour of thin TiN films as discussed in Section S15.1 in the Supplemental Material [40].

In conclusion, we showed that in thin superconducting films, close to the superconducting-to-insulating transition, the scaling  $dT_c(R_s)$  describes the relationships between the film properties. We demonstrated this scaling for the films grown by us and showed that it fits our data better than the previously proposed scaling for  $T_c$  in thin films. Moreover, by examining the data existing in the literature, we demonstrated the universality of this scaling. We quantified the scaling with a power law and supplied possible explanations of its origin. Furthermore, using this scaling, we presented a method to evaluate the quality of a grown film as well as to estimate its  $T_c$ , assisting the control of thin superconducting films, and hence expediting the development of miniaturised superconducting devices and the research of superconductivity at low dimensions. In addition, because existing theories of metallic thin films relating  $R_s$  (or  $\rho$ ) and  $d$  do not involve  $T_c$ , while our

finding does, our result may help understanding better metallic thin films more generally. Finally, the inclusive database formed to allow quantitative analysis of the existing data from the literature can be used for further investigation of the universality of superconductivity in thin films.

### **Acknowledgements:**

The authors would like to thank Terry P. Orlando, Mehran Kardar, Teunis M. Klapwijk, Bertrand I. Halperin, Patrick A. Lee, Leonid S. Levitov, Yosef Imry, Biaobing Jin, Karen Michaeli, Eduard Driessen, Pieter Jan C. J. Coumou, Emanuele G. Dalla Torre, Baruch Barzel and Richard G. Hobbs for very useful discussions. Moreover, they thank the Center for Excitonics, an Energy Frontier Research Center funded by the U.S. Department of Energy, Office of Science, Office of Basic Energy Sciences under award number DE-SC0001088 for funding the project, and Y.I.; A.E.D. and K.A.S. as well as the test apparatus and growth were supported by IARPA (award number FA8650-11-C-7105), while A.M.C. acknowledges fellowship support from the NSF iQuISE program, award number 0801525. The TEM experiment was supported by the U.S. Office of Naval Research (contract #N00014-13-1-0074).

### **Authors contribution:**

Y.I. initiated the study, analysed the data, gathered the published data, grew and characterised NbN films, helped with the TEM study and wrote the paper; CSK helped prepare and conducted the TEM study; A.E.D. helped characterise NbN films and helped gather published data; D.D.F. grew and characterised NbN films; A.M.C. developed the electrical characterisation systems for the NbN films; K.A.S. developed the thickness measurement system for the NbN films and contributed to the paper writing; QZ helped grow NbN films and K.K.B. initiated the study, supervised the

research and helped write the paper. All authors contributed to the discussion and provided feedback on the manuscript.

## **Materials and Methods**

NbN films were sputtered with an ATC ORION Sputtering System, EMOC-380 Power Distribution, and SHQ-15A PID Heater Controller from AJA International Inc. Sputtering conditions were nominal temperature of 800° C; a total pressure of 1.5-6 mTorr; Ar and N<sub>2</sub> flows of 26.5 sccm and 3-7.5 sccm, respectively; a sputtering current of 400 mA; and a target-sample distance of 47 mm. The sputtering time ranged from 45 sec to 300 sec. We used 2" diameter × 0.25" thick Nb 99.95% ExTa targets from Kurt J. Leskor and 10 × 10 × 0.5 mm<sup>3</sup> <100> MgO substrates with both sides polished.  $R_s$  was extracted at ambient conditions from standard 4-probe measurements with a Remington Test LCC stage and a Keithley 2400 SourceMeter.  $T_c$  was determined as the temperature at which  $R_s = (0.9R_s(@20K) + 0.1R_s(@20K))/2$ , where  $R_s(@20K)$  is the measured sheet resistance at 20 K.  $T_c$  was measured in liquid He with an in-house made dipstick (Omegalux KHLV-102/10 flexible heater, a DT-670A LakeShore temperature sensor, and a crycon34 temperature controller). Finally,  $d$  values were measured with an in-house made reflectometer (photodiodes: ThorLabs DET 36A Biased Detectors 350-1100 nm wavelength; LED: 470 nm HI VIS TO-5 IDX:1 OptoDiode Corp. 00-469L-ND; LED Driver: ThorLabs LEDD1B; and Hewlett Packard 34401A Multimeter). TEM images were taken with JEM 2010F by JEOL with a 200 kV beam for several samples from different locations from two films of 14.2 nm and 2.5 nm, all were found to share a similar structure. The selective area electron diffraction images were in great agreement with the fast Fourier transform of the atomic images taken from the same areas. Data presented here are from a film with  $d = 14.2$  nm as measured with the reflectometer (14.6 nm extracted from the TEM image),  $R_s = 75.69 \Omega/\square$ , and  $T_c = 14.24$  K. The

film was sputtered while being held with a thinner sample holder than that used for the set of films presented in Figures 1 and 3, potentially giving rise to a slightly higher substrate temperature.

Previously published data were collected with DataThief III version 1.6 [58]. Whenever the data were collected from several different sources (*i.e.* from different figures within the same work), cross-checking was done, and data points were discarded when the inconsistency was large. Moreover, data were also discarded when it was stated clearly by the authors that the films were too thin to be continuous or to allow reliable measurements (some of the published data were sent by the authors of these publications). A complete list of the collected and presented data, as well as the cross-checking and discussion of each data set are given in the Supplementary Material [40].

#### References:

- [1] M. Tinkham, *Introduction to Superconductivity*, 2nd editio (Dover Publications, New York, 2004), p. 454.
- [2] S. Chakravarty, A. Sudbø, P. W. Anderson, and S. Strong, *Science* **261**, 337 (1993).
- [3] C. C. Homes, S. V Dordevic, M. Strongin, D. A. Bonn, and R. Liang, **430**, 539 (2004).
- [4] Y. Dubi, Y. Meir, and Y. Avishai, *Nature* **449**, 876 (2007).
- [5] V. F. Gantmakher and V. T. Dolgoplov, *Phys. Uspekhi* **180**, 3 (2010).
- [6] A. Shalnikov, *Nature* **142**, 74 (1938).
- [7] L. N. Cooper, *Phys. Rev. Lett.* **6**, 689 (1961).
- [8] M. Beasley, J. Mooij, and T. Orlando, *Phys. Rev. Lett.* **42**, 1165 (1979).
- [9] A. M. Finkel'stein, *Phys. B Condens. Matter* **197**, 636 (1994).
- [10] Y. Guo, Y.-F. Zhang, X.-Y. Bao, T.-Z. Han, Z. Tang, L.-X. Zhang, W.-G. Zhu, E. G. Wang, Q. Niu, Z. Q. Qiu, J.-F. Jia, Z.-X. Zhao, and Q.-K. Xue, *Science* **306**, 1915 (2004).
- [11] A. Shalnikov, *Nature* **142**, 74 (1938).

- [12] R. W. Cohen and B. Abeles, **109**, 444 (1967).
- [13] M. Strongin, R. Thompson, O. Kammerer, and J. Crow, *Phys. Rev. B* **1**, 1078 (1970).
- [14] B. Halperin and D. Nelson, *Phys. Rev. Lett.* **41**, 121 (1978).
- [15] M. W. Johnson and A. M. Kadin, *Phys. Rev.* **57**, 3593 (1998).
- [16] Z. Wang, A. Kawakami, Y. Uzawa, and B. Komiyama, *J. Appl. Phys.* **79**, 7837 (1996).
- [17] S. Miki, Y. Uzawa, A. Kawakami, and Z. Wang, *Electron. Commun. Japan (Part II Electronics)* **85**, 77 (2002).
- [18] S. Ezaki, K. Makise, B. Shinozaki, T. Odo, T. Asano, H. Terai, T. Yamashita, S. Miki, and Z. Wang, *J. Phys. Condens. Matter* **24**, 475702 (2012).
- [19] L. Kang, B. B. Jin, X. Y. Liu, X. Q. Jia, J. Chen, Z. M. Ji, W. W. Xu, P. H. Wu, S. B. Mi, a. Pimenov, Y. J. Wu, and B. G. Wang, *J. Appl. Phys.* **109**, 033908 (2011).
- [20] a. Semenov, B. Günther, U. Böttger, H.-W. Hübers, H. Bartolf, a. Engel, a. Schilling, K. Ilin, M. Siegel, R. Schneider, D. Gerthsen, and N. Gippius, *Phys. Rev. B* **80**, 054510 (2009).
- [21] D. B. Haviland, Y. Liu, and A. M. Goldman, *Phys. Rev. Lett.* **62**, 2180 (1989).
- [22] E. F. C. Driessen, P. C. J. J. Coumou, R. R. Tromp, P. J. de Visser, and T. M. Klapwijk, *Phys. Rev. Lett.* **109**, 107003 (2012).
- [23] P. C. J. J. Coumou, E. F. C. Driessen, J. Bueno, C. Chapelier, and T. M. Klapwijk, *Phys. Rev. B* **88**, 180505(R) (2013).
- [24] H. Kes and C. C. Tsuei, *Phys. Rev. B* **28**, 5126 (1983).
- [25] H. Tashiro, J. Graybeal, D. Tanner, E. Nicol, J. Carbotte, and G. Carr, *Phys. Rev. B* **78**, 014509 (2008).
- [26] S. Turneare, T. Lemberger, and J. Graybeal, *Phys. Rev. B* **63**, 174505 (2001).
- [27] S. Turneare, T. Lemberger, and J. Graybeal, *Phys. Rev. B* **64**, 179901 (2001).
- [28] A. Yazdani and A. Kapitulnik, *Phys. Rev. Lett.* **74**, 3037 (2000).
- [29] H. Raffy, R. Laibowitz, P. Chaudhari, and S. Maekawa, *Phys. Rev. B* **28**, 6607 (1983).
- [30] S. Wolf, D. Gubser, and Y. Imry, *Phys. Rev. Lett.* **42**, 324 (1979).

- [31] K. Fuchs and H. H. Wills, *Math. Proc. Cambridge Philos. Soc.* **34**, 100 (1938).
- [32] P. A. Badoz, A. Briggs, E. Rosencher, F. A. D'Avitaya, and C. D'Anterrosches, *Appl. Phys. Lett.* **51**, 169 (1987).
- [33] T. Sun, B. Yao, A. P. Warren, K. Barmak, M. F. Toney, R. E. Peale, and K. R. Coffey, *Phys. Rev. B* **81**, 155454 (2010).
- [34] B. Sacépé, C. Chapelier, T. Baturina, V. Vinokur, M. Baklanov, and M. Sanquer, *Phys. Rev. Lett.* **101**, 157006 (2008).
- [35] G. N. Gol'tsman, O. Okunev, G. Chulkova, A. Lipatov, A. Semenov, K. Smirnov, B. Voronov, A. Dzardanov, C. Williams, and R. Sobolewski, *Appl. Phys. Lett.* **79**, 705 (2001).
- [36] J. Clarke and F. K. Wilhelm, *Nature* **453**, 1031 (2008).
- [37] F. Najafi, F. Marsili, E. Dauler, R. J. Molnar, and K. K. Berggren, *Appl. Phys. Lett.* **100**, 152602 (2012).
- [38] F. Marsili, F. Bellei, F. Najafi, A. E. Dane, E. A. Dauler, R. J. Molnar, and K. K. Berggren, *Nano Lett.* **12**, 4799 (2012).
- [39] G. N. Gol'tsman, O. Okunev, G. Chulkova, A. Lipatov, A. Semenov, K. Smirnov, B. Voronov, A. Dzardanov, C. Williams, and R. Sobolewski, *Appl. Phys. Lett.* **79**, 705 (2001).
- [40] Supplemental Material is available online at [URL will be inserted by Publisher].
- [41] R. Koushik, S. Kumar, K. R. Amin, M. Mondal, J. Jesudasan, A. Bid, P. Raychaudhuri, and A. Ghosh, *Phys. Rev. Lett.* **111**, 197001 (2013).
- [42] B. Matthias, T. Geballe, and V. Compton, *Rev. Mod. Phys.* **35**, 1 (1963).
- [43] K. M. Rosfjord, J. K. W. Yang, E. A. Dauler, A. J. Kerman, V. Anant, B. M. Voronov, G. N. Gol'tsman, and K. K. Berggren, *Opt. Express* **14**, 527 (2006).
- [44] F. Marsili, F. Najafi, E. Dauler, F. Bellei, X. Hu, M. Csete, R. J. Molnar, and K. K. Berggren, *Nano Lett.* **11**, 2048 (2011).
- [45] W. McMillan, *Phys. Rev.* **167**, 331 (1968).
- [46] P. B. Allen, *Phys. Rev. B* **12**, 905 (1975).
- [47] T. I. Baturina, S. V. Postolova, A. Y. Mironov, A. Glatz, M. R. Baklanov, and V. M. Vinokur, *EPL (Europhysics Lett.)* **97**, 17012 (2012).

- [48] J. M. Graybeal and M. R. Beasley, *Phys. Rev. B* **29**, 4167 (1984).
- [49] A. V. Pogrebnyakov, J. M. Redwing, J. E. Jones, X. X. Xi, S. Y. Xu, Q. Li, V. Vaithyanathan, and D. G. Schlom, *Appl. Phys. Lett.* **82**, 4319 (2003).
- [50] H. M. Jaeger, D. B. Haviland, B. G. Orr, and A. M. Goldman, *Phys. Rev. B* **40**, 182 (1989).
- [51] T. Orlando, E. McNiff, S. Foner, and M. Beasley, *Phys. Rev. B* **19**, 4545 (1979).
- [52] L. Fàbrega, a Camón, I. Fernández-Martínez, J. Sesé, M. Parra-Borderías, O. Gil, R. González-Arrabal, J. L. Costa-Krämer, and F. Briones, *Supercond. Sci. Technol.* **24**, 075014 (2011).
- [53] A. Gubin, K. Il'in, S. Vitusevich, M. Siegel, and N. Klein, *Phys. Rev. B* **72**, 064503 (2005).
- [54] T. I. Baturina and S. V. Postolova, in *Int. Work. Strongly Disord. Supercond. Supercond. Insul. Transit.* (2104), Villard de Lans, France.
- [55] J. M. Graybeal, *Phys. B+C* **135**, 113 (1985).
- [56] Q. Zhao, A. McCaughan, F. Bellei, F. Najafi, D. De Fazio, A. Dane, Y. Ivry, and K. K. Berggren, *Appl. Phys. Lett.* **103**, 142602 (2013).
- [57] Q. Zhao, A. McCaughan, A. Dane, F. Najafi, F. Bellei, D. De Fazio, K. Sunter, Y. Ivry, and K. K. Berggren, *arXiv:1408.1124* (2014).
- [58] DataTheif III version 1.6, [Http://datathief.org](http://datathief.org), B. Tummars, (2006).